Mathematical Models of Gear Rattle in Roots blower Vacuum Pumps

Joanna Mason [*], *Martin Homer*, *R. Eddie Wilson*,

Bristol Centre for Applied Nonlinear Mathematics, University of Bristol, BS8 1TR.

Abstract

This paper is concerned with the modelling of gear rattle in Roots blower vacuum pumps. Analysis of experimental data reveals that the source of the noise and vibration problem is the backlash nonlinearity due to gear teeth losing and re-establishing contact. We develop non-smooth ordinary differential equation models for the dynamics of the pump. The models include a time-dependent forcing term which arises from the imperfect, eccentric mounting of the gears. We use a combination of explicit construction, asymptotic methods and numerical techniques to classify complicated dynamic behaviour in realistic parametric regimes. We first present a linear analysis of motions where the gears do not lose contact, and develop upper bounds on eccentricity for quiet operation. We then develop a nonlinear analysis of 'backlash oscillations', where the gears lose and re-establish contact, corresponding to noisy pump operation. It is found that noisy solutions can coexist with silent ones, explaining why geared systems can rattle intermittently. We then consider several possible design solutions, and show their implications for pump design in terms of the existence and stability of silent and noisy solutions. Finally, we present conclusions and possibilities for future work.

1 Introduction

Recent increases in the sizes and operating speeds of Roots blower vacuum pumps have led to intermittent noise and vibration problems in their gearing mechanism. A small amount of play between gears is essential to ensure that they will not jam. This means that there is always a gap between the trailing face of one tooth and the leading face of the next tooth, which is known as the backlash width. Because the gear wheels can consequently lose contact, there is a range of relative rotational displacements for which there is no restoring torque between the gears: this effect is known as freeplay. A tiny amount of eccentricity in the mounting of the gears introduces a forcing effect which causes the gear teeth to repeatedly lose and re-establish contact. The key design challenge is therefore to change the machine design so that it is less susceptible to noisy operation driven by eccentricity.

The main theoretical advance presented is the extension of the second order model in Halse *et al.* [2, 3], to a third order model where the moments of inertia of the two shafts are not necessarily equal. We investigate the effect that breaking the symmetry has on the analytical bounds for the existence of various types of solution, and hence the critical eccentricity, and conclusions are drawn for machine design.

1.1 Model formulation

A typical Roots blower vacuum pump [1, 4, 7, 8] consists of two involute steel rotors which are rigidly attached to counter-rotating parallel shafts. The X-shaft is driven by an electric motor, while the Y-shaft

[*]Gratefully acknowledges the support of a CASE award from BOC Edwards Ltd. and EPSRC.

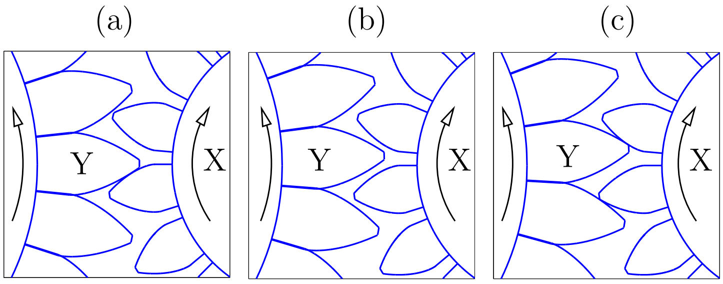

Fig. 1: The three modes of gear meshing (full details are given in [6]). From left to right: (a) X drives Y, (b) Freeplay, (c) Y drives X (torque reversal).

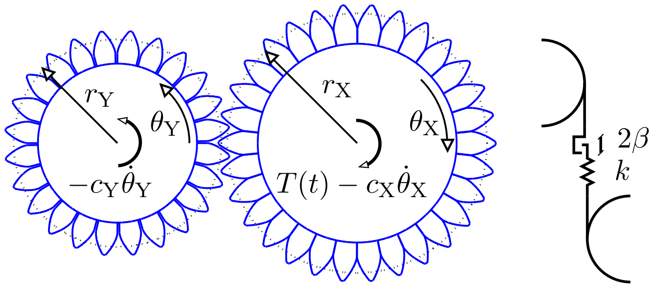

Fig. 2: The external torques acting on the shafts of meshing gears. The right hand side drawing illustrates the interaction force between the gears.

is driven by means of a 1:1 gearing mechanism. When the gear teeth are in contact, we use a lumped approach and we suppose that each assembly deforms according to Hooke's Law.

In quiet ('normal') operation, the gears remain in permanent linear contact (PLC), as shown in Figure 1(a). However in noisy operation, the gears lose contact, and the impact when the gears re-establish contact is audible. This is known as a backlash oscillation. There are in fact two broad types of backlash oscillations. Starting from state (a) in Figure 1, the system can pass through state (b) to state (c) and back again. Alternatively, the system can simply oscillate between states (a) and (b). We believe that the first type of oscillations are the noisiest; in any case torque reversal is highly undesirable.

We consider a model of two meshing spur gears and the external forces acting on the two shafts, as shown schematically in Figure 2. The X-shaft is driven by a motor torque $T(t)$. The moments of inertia of the fully assembled shafts are denoted by $I_{\mathrm{X,Y}}$, and $r_{\mathrm{X,Y}}$ denote the radii of the pitch circle at which contact occurs between the X and Y gears; we assume $r_{\mathrm{X}} = r_{\mathrm{Y}}$. The angular displacements $\theta_{\mathrm{X,Y}}$ have directions chosen so that both coordinates increase in time. Both the X and Y-shafts suffer resistive torques against the direction of motion, given by $c_{\mathrm{X,Y}}\dot{\theta}_{\mathrm{X,Y}}$, where $c_{\mathrm{X,Y}}$ are linear damping coefficients. The relative rotational displacement is defined generally by $r_{\mathrm{X}}\theta_{\mathrm{X}} - r_{\mathrm{Y}}\theta_{\mathrm{Y}}$. Here we focus on the special case $r_{\mathrm{X}} = r_{\mathrm{Y}}$, for which we work with the non-dimensional relative rotational displacement $\Theta := \theta_{\mathrm{X}} - \theta_{\mathrm{Y}}$. The stiffness coefficient k is a measure of the lumped torsional rigidity of the shaft assemblies. Each gear experiences a restoring normal reaction force kB, which acts normal to the shafts, and which is dependent on the relative position of the gear teeth. Here B is a nonlinear backlash function that consists of three linear components:

$$B(\Theta) = \begin{cases} \Theta - \beta, & \Theta > \beta, & \text{(X drives Y)} \\ 0, & |\Theta| < \beta, & \text{(freeplay)} \\ \Theta + \beta, & \Theta < -\beta. & \text{(Y drives X)} \end{cases} \tag{1}$$

1.2 Equations of motion

We apply Newton's second law of motion in angular coordinates to derive equations of motion for the two shaft assemblies. For the X and Y-shaft assemblies respectively we have

$$I_{\mathrm{X}}\ddot{\theta}_{\mathrm{X}} + c_{\mathrm{X}}\dot{\theta}_{\mathrm{X}} + r_{\mathrm{X}}kB(r_{\mathrm{X}}\theta_{\mathrm{X}} - r_{\mathrm{Y}}\theta_{\mathrm{Y}} + e(t)) = T(t), \tag{2}$$

$$I_{\mathrm{Y}}\ddot{\theta}_{\mathrm{Y}} + c_{\mathrm{Y}}\dot{\theta}_{\mathrm{Y}} - r_{\mathrm{Y}}kB(r_{\mathrm{X}}\theta_{\mathrm{X}} - r_{\mathrm{Y}}\theta_{\mathrm{Y}} + e(t)) = 0, \tag{3}$$

where $e(t)$ is the oscillatory correction for eccentricity and dots denote differentiation with respect to time. We model the total motor torque T by $T(t) = \overline{T} + \gamma \cos(2\pi n\tau + \xi)$, where $\overline{T}$ is the mean motor torque and γ is the amplitude of a ripple component, due to the imperfect symmetry of the armature. The mean torque $\overline{T}$ balances with the drag terms when the machine is running steadily, and so it need not be given as a separate parameter. Providing that $c_x/I_x = c_y/I_y$ we can reduce (2) and (3) to a single non-autonomous second-order differential equation for the relative rotational displacment measured at the pitch circle $\Phi = \theta_X - \theta_Y + e(t)$. By non-dimensionalising with the rotation period, we find that

$$\Phi'' + \delta\Phi' + 2\kappa B(\Phi) = 4\pi\delta - 4\pi^2\varepsilon\cos(2\pi\tau) - 2\pi\delta\varepsilon\sin(2\pi\tau) + \gamma\cos(2\pi n\tau + \xi), \tag{4}$$

where $'$ denotes differentiation with respect to non-dimensional time τ. Typical values of the non-dimensional parameters are $\delta \sim \beta \sim \varepsilon \sim \mathcal{O}(10^{-4})$ and $\kappa \sim \mathcal{O}(10^3)$. We note for future reference that δ and κ are inversely proportional to I. The ripple component γ of the mean motor torque $4\pi\delta$ is very small, therefore, for the remainder of our work we neglect torque ripple and concentrate on the effect of eccentricity only. We note that the rescaled damping δ, half backlash width β and eccentricity parameter ε are good candidates for use as small parameters in perturbation analysis. In comparison, the rescaled stiffness parameter κ is large.

1.2.1 Two degree of freedom dimensionless model

The single degree of freedom (d.o.f.) model requires that the ratio of the moments of inertia and damping coefficients of the X and Y shafts are equal. We now extend the scope of our model by allowing the quantities to differ; in this case, θ_X and θ_Y are independent coordinates. We choose a non-dimensional parameter $\eta \in (-1, 1)$, to measure the broken symmetry, so that

$$\frac{I_X}{\overline{I}} = 1 + \eta, \qquad \text{and} \qquad \frac{I_Y}{\overline{I}} = 1 - \eta, \qquad \text{where } \overline{I} = \frac{I_X + I_Y}{2}. \tag{5}$$

After non-dimensionalisation as before, it is possible to re-write the pair of coupled second order ODEs as a system of three first order equations by introducing new coordinates, $(\Phi,\, \Psi,\, Z)$, where $\Phi = \theta_x - \theta_y + e(t)$ is as before, $\Psi = \Phi'$ and $Z = \theta_X' + \theta_Y'$. We now have

$$\begin{pmatrix} 1 & 0 & 0 \\ 0 & 1 & \eta \\ 0 & \eta & 1 \end{pmatrix} \begin{pmatrix} \Phi' \\ \Psi' \\ Z' \end{pmatrix} = \begin{pmatrix} 0 & 1 & 0 \\ 0 & -\delta & 0 \\ 0 & 0 & -\delta \end{pmatrix} \begin{pmatrix} \Phi \\ \Psi \\ Z \end{pmatrix} + \begin{pmatrix} 0 \\ 4\pi\delta + e''(\tau) + \delta e'(\tau) - 2\kappa B(\Phi) \\ 4\pi\delta + \eta e''(\tau) \end{pmatrix}. \tag{6}$$

Note that δ, ε and κ have exactly the same values as for the one d.o.f. model.

2 Permanent Linear Contact Solutions

Solutions where the gears remain permanently in contact are highly desirable; we wish to find bounds on parameters for their existence. Equation (4) for Φ in the PLC region is linear and can be solved exactly. We must then apply an *a posteriori* check for the validity of solutions, namely that $\Phi(\tau) > \beta$ for all τ. This provides us with a bound for eccentricity:

$$\varepsilon < \varepsilon_{\text{crit}}^{\text{1d.o.f.}} := \frac{2\delta}{\kappa}\sqrt{\frac{(\kappa - 2\pi^2)^2 + \pi^2\delta^2}{4\pi^2 + \delta^2}}, \tag{7}$$

above which silent solutions are destroyed. As $\kappa \to \infty$ (motivated by physical parameters of real machines) we have

$$\varepsilon_{\text{crit}} \sim \frac{\delta}{\pi} + O(\delta^3). \tag{8}$$

Typical measured eccentricities are of the same order of magnitude as the calculated critical eccentricity; this could explain the experimental observations that the same machine can behave inconsistently and ‘identical’ machines behave differently. Increasing inertia, however, decreases δ and will make rattle more likely; we therefore wish to find design solutions to increase $\varepsilon_{\text{crit}}$. Therefore, we now examine the effect of breaking symmetry.

We write equation (6) in the form:

$$\boldsymbol{M}\boldsymbol{u}' = \boldsymbol{A}\boldsymbol{u} + \boldsymbol{b}_1 - \Re\{\boldsymbol{b}_2 \exp 2\pi\tau\mathrm{i}\}, \tag{9}$$

where $\Re$ denotes the real part, i the square root of -1 and $e(\tau) = \Re\{\varepsilon \exp 2\pi\tau\mathrm{i}\}$ is the eccentricity term. We solve the ODE (9), and apply the *a posteriori* check to find the bound

$$\varepsilon < \varepsilon_{\text{crit}}^{\text{2d.o.f.}} = \frac{2\delta}{\kappa}\sqrt{\frac{((\kappa-2\pi^2)^2+\pi^2\delta^2)+\frac{8\pi^4\eta^2}{4\pi^2+\delta^2}\left(2(\kappa-2\pi^2)+\delta^2+2\pi\eta^2\right)}{(4\pi^2+\delta^2)+\frac{8\pi^2\eta^2}{4\pi^2+\delta^2}\left((4\pi^2-\delta^2)-2\pi^2\eta^2\right)}}, \tag{10}$$

for the existence of PLC solutions. Note that for $\eta = 0$, $\varepsilon_{\text{crit}}^{\text{2d.o.f.}} = \varepsilon_{\text{crit}}^{\text{1d.o.f.}}$ as required. Expanding (10) as a binomial series in small η, for fixed δ and κ, gives

$$\varepsilon_{\text{crit}} = \varepsilon_{\text{crit}}^{\text{1d.o.f.}}(1+\eta^2+O(\eta^4)). \tag{11}$$

Hence for small η, breaking the symmetry by removing mass from one shaft and adding it to the other increases $\varepsilon_{\text{crit}}$ (a desirable effect). The advantage of the η parameter is that it allows easy manipulation of the equations of motion and does not change the values of the other nondimensional parameters. However it is more physically interesting to investigate the effect of adding/removing mass to just one shaft, or equally to both shafts. We thus introduce two new nondimensional variables μ and ν: μ measures half the ratio of mass added/removed to *either* the X or Y-shaft, while ν measures the ratio of mass added/removed to *each* shaft. Note that the parameters ν and μ result in the same total change in mass.

We substitute expressions for μ and ν into (10) (with suitably modified damping and stiffness parameters due to the change in total mass) and then expand as a binomial series in small μ, ν respectively for fixed δ and κ as above, to give

$$\varepsilon_{\text{crit}} = \varepsilon_{\text{crit}}^{\text{1d.o.f.}}(1-\mu+2\mu^2+O(\mu^3)), \tag{12}$$

and

$$\varepsilon_{\text{crit}} = \varepsilon_{\text{crit}}^{\text{1d.o.f.}}(1-\nu+\nu^2+O(\nu^3)). \tag{13}$$

Thus (for small μ and ν) it is better to remove mass from one shaft rather than half the amount of mass from both the X and Y-shafts, but the improvement is a second order effect.

3 Conditions for Noisy Operation

Numerical simulations of the initial value problems (IVP) (4), (6) reveal a very rich structure of co-existing stable solutions. Analysis for the one d.o.f. model shows that there are many stable rattling periodic orbits that can coexist with quiet operation; simulations suggest that this is also true in the two d.o.f. model. In fact for some parameter values it seems that noisy solutions predominate. We would like to understand the conditions of existence for these rattling solutions, with a view to exploring whether or not we can destroy them for certain choices of parameters. It was shown in [2, 3] that, to leading order, existence and stability criteria are identical for the finite and infinite stiffness models in the limit $\kappa \to \infty$, thus for convenience we consider only the impacting model of backlash here.

We use the notation introduced in [2, 3] to identify different types of periodic solution. We let $P(m, n^+, n^-)$ denote a periodic solution, of period $m \in \mathbb{Z}$, where $n^\pm$ denote the number of times per period that the orbit contacts the $\Phi = \pm\beta$ boundaries respectively.

3.1 $P(m, 1, 0)$ solutions

We begin by considering solutions of type $P(m, 1, 0)$, which repeat once every m periods of the forcing, hit the $\Phi = +\beta$ boundary once per period and never contact the $\Phi = -\beta$ boundary (see Figure 3).

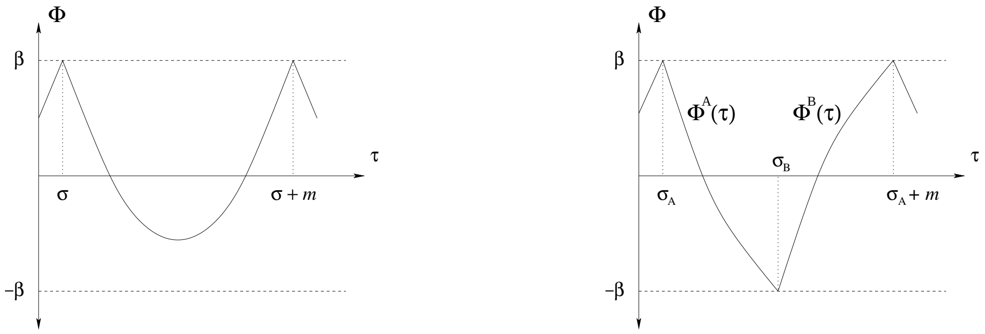

Fig. 3: Sketches of $P(m,1,0)$ and $P(m,1,1)$ orbits respectively. The LHS picture illustrates the impacts at the $+\beta$ boundary, at unknown times σ and $\sigma+m$. The RHS picture illustrates the $\pm\beta$ impacts at $\sigma_{\rm A}$ and $\sigma_{\rm B}$ respectively.

Our general method for solution construction is as follows. We solve the differential equation (6) in the freeplay region and find explicit expressions for Φ, Ψ and Z. We then patch solution segments together with the impact and periodicity conditions.

With reference to Figure 3 our solution makes contact with the $+\beta$ boundary at some initial unknown time σ, with velocity $-v$; the periodicity condition then implies that our solution impacts the $+\beta$ boundary again at some time $\sigma+m$ with velocity v. Hence:

$$\Phi(\sigma)=\beta, \qquad \Psi(\sigma)=-v, \tag{14}$$

$$\Phi(\sigma+m)=\beta, \qquad \Psi(\sigma+m)=v. \tag{15}$$

Conservation of angular momentum also implies that

$$Z(\sigma)=Z(\sigma+m)+2\eta v. \tag{16}$$

By applying conditions (14)–(16) we obtain a system in the form, $\boldsymbol{Ac}=\boldsymbol{b}$ to solve for the five unknowns c_1, c_2, c_3, v and σ,

$$\begin{pmatrix} 1 & e^{-\lambda_-\sigma} & e^{-\lambda_+\sigma} & 0 \\ 1 & e^{-\lambda_-(\sigma+m)} & e^{-\lambda_+(\sigma+m)} & 0 \\ 0 & -\lambda_-e^{-\lambda_-\sigma} & -\lambda_+e^{-\lambda_+\sigma} & 1 \\ 0 & -\lambda_-e^{-\lambda_-(\sigma+m)} & -\lambda_+e^{-\lambda_+(\sigma+m)} & -1 \\ 0 & \lambda_-e^{-\lambda_-\sigma}\left(1-e^{-\lambda_-m}\right) & -\lambda_+e^{-\lambda_+\sigma}\left(1-e^{-\lambda_+m}\right) & -2\eta \end{pmatrix}\begin{pmatrix} c_1 \\ c_2 \\ c_3 \\ v \end{pmatrix} = \begin{pmatrix} \beta-4\pi\sigma-\varepsilon\cos(2\pi\sigma) \\ \beta-4\pi(\sigma+m)-\varepsilon\cos(2\pi\sigma) \\ -4\pi+2\pi\varepsilon\sin(2\pi\sigma) \\ -4\pi+2\pi\varepsilon\sin(2\pi\sigma) \\ 0 \end{pmatrix}, \tag{17}$$

where $\boldsymbol{c}$ is a vector consisting of $\boldsymbol{v}$ and the constants of integration (that occur in the solutions for Φ, Ψ and Z) and $\lambda_\pm=\delta/(1\pm\eta)$. We now find a matrix $\boldsymbol{P}$ such that $\boldsymbol{PA}$ is in echelon form, which gives us expressions for c_1, c_2, c_3 and v, and generates an algebraic constraint on the impact time σ.

3.1.1 Existence and stability of solutions

When following the above procedure, we find that the impact time σ takes the form

$$\sigma=\frac{1}{2\pi}\sin^{-1}\left[\frac{1}{\varepsilon}\left(2-\frac{\delta m}{2(1-\eta)}\coth\left(\frac{\delta m}{2(1-\eta)}\right)-\frac{\delta m}{2(1+\eta)}\coth\left(\frac{\delta m}{2(1+\eta)}\right)\right)\right]. \tag{18}$$

There are two admissible solutions to (18); we expand them in terms of the small parameter δ to give:

$$\sigma=\begin{cases} \dfrac{-\delta^2m^2(1+\eta^2)}{12\pi\varepsilon(1-\eta^2)^2}+O(\delta^4) & : \quad \text{for the in phase solution,} \\ \dfrac{1}{2}+\dfrac{\delta^2m^2(1+\eta^2)}{12\pi\varepsilon(1-\eta^2)^2}+O(\delta^4) & : \quad \text{for the out of phase solution.} \end{cases} \tag{19}$$

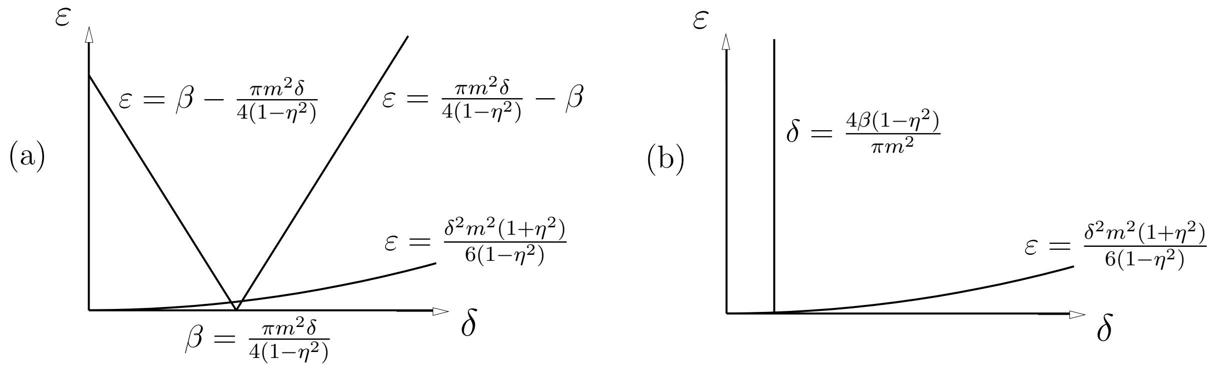

Fig. 4: Sketches of the existence bounds for the $P(m, 1, 0)$ solutions: (a) m odd and (b) m even. The regions of existence are described by the inequalities in (20), (22) and (23).

The $P(m, 1, 0)$ solutions do not exist if the argument of the arcsin function in (18) exceeds one in modulus. This gives us a condition on eccentricity:

$$\varepsilon < \varepsilon_{\rm crit} := \frac{\delta^2 m^2 (1+\eta^2)}{6(1-\eta^2)} + O(\delta^4), \tag{20}$$

for the existence of simple $P(m, 1, 0)$ solutions. We must also check that the solution trajectory does not hit the boundary $\Phi = -\beta$. To determine this we must find the minimum displacement; we thus require $\hat{\tau}$ such that $\Psi(\hat{\tau}) = 0$, and we try a power series solution in the form

$$\hat{\tau} = \sigma + \frac{m}{2} + \hat{\tau}_0 + \hat{\tau}_1\delta + O(\delta^2). \tag{21}$$

We have four cases corresponding to in phase/out of phase solution and m odd/even. In each case we solve for the coefficients $\hat{\tau}_i$, substitute these expressions for $\hat{\tau}$ into the condition $\Phi(\hat{\tau}) > -\beta$ and expand this as a series as well. For the in phase solution ($\sigma \approx 0$) not to contact the lower boundary we require

$$\beta > \begin{cases} \varepsilon + \frac{\pi m^2\delta}{4(1-\eta^2)} + O(\delta^2) & : \quad m \text{ odd}, \\ \frac{\pi m^2\delta}{4(1-\eta^2)} + O(\delta^2) & : \quad m \text{ even}, \end{cases} \tag{22}$$

and for the out of phase solution ($\sigma \approx \frac{1}{2}$) not to contact the lower boundary we require

$$\beta > \begin{cases} \frac{\pi m^2\delta}{4(1-\eta^2)} - \varepsilon + O(\delta^2) & : \quad m \text{ odd}, \\ \frac{\pi m^2\delta}{4(1-\eta^2)} + O(\delta^2) & : \quad m \text{ even}. \end{cases} \tag{23}$$

In Figure 4 we have plotted the existence bounds found in (20), (22) and (23) of eccentricity against damping. Note that when the symmetry breaking parameter $\eta = 0$ we recover the bounds for the one d.o.f. model. From this we conclude that increasing η only increases the bounds on ε by a higher order amount. Unfortunately, the upper bound on ε, $\left(\varepsilon = \frac{\delta^2 m^2(1+\eta^2)}{6(1-\eta^2)}\right)$ is still of order $\mathcal{O}(\delta^2)$.

3.2 $P(m, 1, 1)$ Solutions

We now proceed to show how one might examine noisier, less desirable, $P(m, 1, 1)$ solutions that visit all three regimes, thus impacting both $\pm\beta$ boundaries. The overall aim is to find existence bounds for these noisy solutions, and therefore determine how they can be eliminated. We write the solution Φ as the combination of these two parts so that

$$\Phi(\tau) = \begin{cases} \Phi^{\rm A}(\tau), & \sigma_{\rm A} < \tau < \sigma_{\rm B}, \\ \Phi^{\rm B}(\tau), & \sigma_{\rm B} < \tau < \sigma_{\rm A} + m, \end{cases} \tag{24}$$

(and similarly for Ψ and Z); see Figure 3. For this calculation we shall consider period one solutions, i.e., $m = 1$. The $\Phi^{\rm A}$ section of the solution makes contact with the $\pm\beta$ boundaries at some unknown times $\sigma_{\rm A}$ and $\sigma_{\rm B}$, while the $\Phi^{\rm B}$ section of the solution makes contact with the $\pm\beta$ boundaries at some unknown times $\sigma_{\rm B}$ and $\sigma_{\rm A}+1$, hence

$$\Phi^{\rm A}(\sigma_{\rm A}) = \beta, \qquad \Phi^{\rm A}(\sigma_{\rm B}) = -\beta, \tag{25}$$

$$\Phi^{\rm B}(\sigma_{\rm B}) = -\beta, \qquad \Phi^{\rm B}(\sigma_{\rm A}+1) = \beta. \tag{26}$$

Assuming Newtonian impact, with coefficient of restitution equal to one, we obtain

$$\Psi^{\rm A}(\sigma_{\rm A}) = -\Psi^{\rm B}(\sigma_{\rm A}+1), \qquad \Psi^{\rm A}(\sigma_{\rm B}) = -\Psi^{\rm B}(\sigma_{\rm B}). \tag{27}$$

Further, conservation of angular momentum implies that

$$\begin{aligned} Z^{\rm A}(\sigma_{\rm A}) + \eta\Psi^{\rm A}(\sigma_{\rm A}) &= Z^{\rm B}(\sigma_{\rm A}+1) + \eta\Psi^{\rm B}(\sigma_{\rm A}+1), &(28)\\ Z^{\rm A}(\sigma_{\rm B}) + \eta\Psi^{\rm A}(\sigma_{\rm B}) &= Z^{\rm B}(\sigma_{\rm B}) + \eta\Psi^{\rm B}(\sigma_{\rm B}), &(29)\end{aligned}$$

must be met. By applying the conditions (25)–(29) we obtain a system in the form $\boldsymbol{Ac}=\boldsymbol{b}$,

$$\begin{pmatrix} 1 & e^{-\lambda_-\sigma_{\rm A}} & e^{-\lambda_+\sigma_{\rm A}} & 0 & 0 & 0 \\ 1 & e^{-\lambda_-\sigma_{\rm B}} & e^{-\lambda_+\sigma_{\rm B}} & 0 & 0 & 0 \\ 0 & 0 & 0 & 1 & e^{-\lambda_-\sigma_{\rm B}} & e^{-\lambda_+\sigma_{\rm B}} \\ 0 & 0 & 0 & 1 & e^{-\lambda_-(\sigma_{\rm A}+1)} & e^{-\lambda_+(\sigma_{\rm A}+1)} \\ 0 & e^{-\lambda_-\sigma_{\rm A}} & -e^{-\lambda_+\sigma_{\rm A}} & 0 & -e^{-\lambda_-(\sigma_{\rm A}+1)} & e^{-\lambda_+(\sigma_{\rm A}+1)} \\ 0 & e^{-\lambda_-\sigma_{\rm B}} & -e^{-\lambda_+\sigma_{\rm B}} & 0 & -e^{-\lambda_-\sigma_{\rm B}} & e^{-\lambda_+\sigma_{\rm B}} \\ 0 & \lambda_- e^{-\lambda_-\sigma_{\rm A}} & \lambda_+ e^{-\lambda_+\sigma_{\rm A}} & 0 & \lambda_- e^{-\lambda_-(\sigma_{\rm A}+1)} & \lambda_+ e^{-\lambda_+(\sigma_{\rm A}+1)} \\ 0 & \lambda_- e^{-\lambda_-\sigma_{\rm B}} & \lambda_+ e^{-\lambda_+\sigma_{\rm B}} & 0 & \lambda_- e^{-\lambda_-\sigma_{\rm B}} & \lambda_+ e^{-\lambda_+\sigma_{\rm B}} \end{pmatrix} \begin{pmatrix} c_1^{\rm A} \\ c_2^{\rm A} \\ c_3^{\rm A} \\ c_1^{\rm B} \\ c_2^{\rm B} \\ c_3^{\rm B} \end{pmatrix}$$

$$= \begin{pmatrix} \beta - 4\pi\sigma_{\rm A} - \varepsilon\cos 2\pi\sigma_{\rm A} \\ -\beta - 4\pi\sigma_{\rm B} - \varepsilon\cos 2\pi\sigma_{\rm B} \\ -\beta - 4\pi\sigma_{\rm B} - \varepsilon\cos 2\pi\sigma_{\rm B} \\ \beta - 4\pi(\sigma_{\rm A}+1) - \varepsilon\cos 2\pi\sigma_{\rm A} \\ 0 \\ 0 \\ 8\pi - 4\pi\varepsilon\sin 2\pi\sigma_{\rm A} \\ 8\pi - 4\pi\varepsilon\sin 2\pi\sigma_{\rm B} \end{pmatrix}, \tag{30}$$

where $\boldsymbol{c}$ is a vector of the constants of integration. This system of equations can now be solved as before to determine the integration constants $c_1^{\rm A,B}$, $c_2^{\rm A,B}$, $c_3^{\rm A,B}$ and impact times $\sigma_{\rm A,B}$. As the expressions for $\sigma_{\rm A,B}$ are not solvable in closed form, it is necessary to resort to a numerical root finding procedure to find the impact times. Once the solutions have been found, as for the $P(m,1,0)$ case, a retrospective check has to be made to ensure that the constructed solution is in the correct regimes at the right times. The aim would then be to find conditions on the symmetry-breaking parameters, to determine how this noisy type of solution can be destroyed and replaced by quieter single-contact solutions. This analysis remains for future work. We can, however, determine stability numerically using an initial value solver written in Matlab. We find that typically the in-phase solution is unstable, and the out-of-phase solution is stable. Some outputs are shown in Figure 5.

4 Conclusions

In this paper we have considered a mathematical model of noise and vibration in Roots blower vacuum pumps. We have extended the work carried out by Halse *et al* [2, 3], by constructing a full two d.o.f. model, and investigated the effects of breaking the symmetry between the two shafts. In particular, we derived analytic bounds for the existence of various classes of periodic solution as a function of parameters.

We discovered that breaking the symmetry of the system by removing mass increases the critical value of eccentricity (above which silent solutions cannot exist). Unfortunately one is very limited in

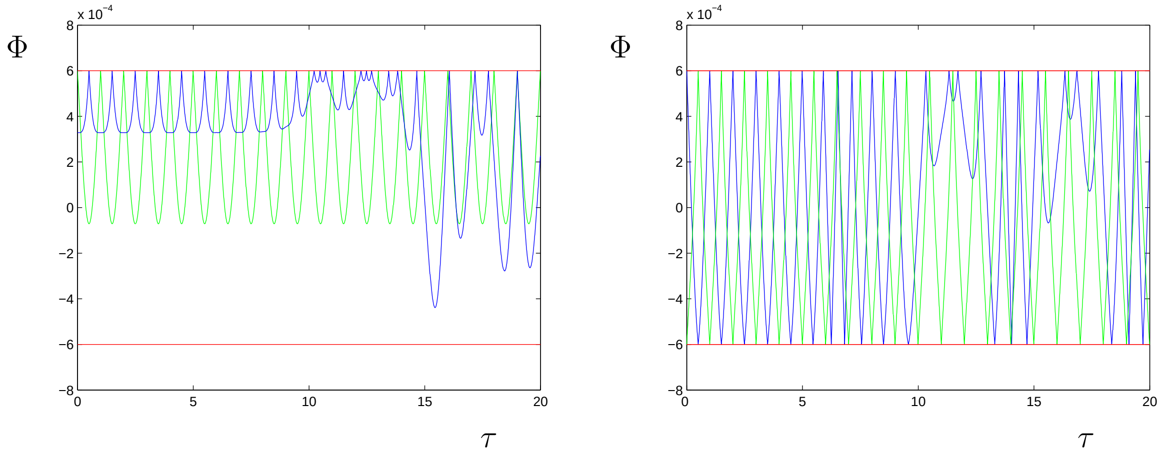

Fig. 5: Simulations of $P(m,1,0)$ and $P(m,1,1)$ solutions respectively for the one d.o.f. model. The horizontal lines illustrate the $\pm\beta$ boundaries. Grey shows the stable solution, whilst black shows a simulation close to the co-existing unstable solution.

how much mass one can remove from such a machine, without compromising its structural integrity. We found that breaking the symmetry of the system solely by adding mass to one or both shafts lowers the existence bound for 'silent' PLC solutions. In future we will expand the work of Section 3 to gain a better understanding of the coexistence of solutions and their stability domains to generate a formal bifurcation analysis.

Numerical simulations of the IVP suggest that solutions are very sensitive to initial data. A possible design solution may be to control initial data in order to select particular solutions, or actively control the motion to isolate desirable trajectories. Future work will include the computation of the basins of attraction, i.e., which starting configurations end up at which (stable) periodic solutions. Further study will also involve the investigation of other design solutions, such as the use of spring-loaded anti-backlash gears. Mathematical models of these new types of system will involve more degrees of freedom and will be more complicated than any existing mathematical treatment of backlash systems.

References

[1] M.H. Hablanian. Design and performance of oil-free pumps. *Vacuum*, 41:1814–1818, 1990.

[2] C.K. Halse. *Nonlinear Dynamics of the Automotive Driveline*. PhD thesis, University of Bristol, 2004.

[3] C.K. Halse, R.E. Wilson, M.E. Homer, and M. di Bernardo. Coexisting solutions and bifurcations in mechanical oscillators with backlash, preprint, 2006.

[4] W.T. Holmes. *Plane Geometry of Rotors in Pumps and Gears*. The Scientific Publishing Company, 1978.

[5] J.F. Mason. Mathematical modelling of gear rattle in dual-shaft vacuum pumps. Master's thesis, University of Bristol, 2004.

[6] H.E. Merritt. *Gear Engineering*. Pitman Publishing, 1971.

[7] A.P. Troup and N.T.M. Dennis. Six years of "dry pumping": A review of experiences and issues. *J. Vac. Sci. Technol. A*, 9:2048–2052, 1990.

[8] H. Wycliffe. Mechanical high-vacuum pumps with oil-free swept volume. *J. Vac. Sci. Technol. A*, 5:2608–2611, 1987.